

Learning Discriminant Direction Binary Palmprint Descriptor

Lunke Fei, Bob Zhang, *Member, IEEE*, Yong Xu, *Senior Member, IEEE*, Zhenhua Guo, *Member, IEEE*, Jie Wen, Wei Jia, *Member, IEEE*,

Abstract—Palmprint directions have been proved to be one of the most effective features for palmprint recognition. However, most existing direction-based palmprint descriptors are hand-craft designed and require strong prior knowledge. In this paper, we propose a discriminant direction binary code learning method for palmprint recognition. Specifically, for each palmprint image, we first calculate the convolutions of the direction-based templates and palmprint, and form informative convolution difference vectors by computing the convolution difference between the neighboring directions. Then, we propose a simple yet effective model to learn feature mapping functions that can project these convolution difference vectors into discriminant direction binary codes (DDBC). For all training samples, (1) the variance of the learned binary codes is maximized, (2) intra-class distance of the binary codes is minimized and (3) the inter-class distance of the binary codes is maximized. Finally, we cluster the block-wise histograms of DDBC forming the discriminant direction binary palmprint descriptor for palmprint recognition. Experimental results on four challenging contactless palmprint databases clearly demonstrate the effectiveness of the proposed method.

Index Terms—Palmprint recognition, Direction feature learning, Discriminant direction binary code, Biometrics.

I. INTRODUCTION

BIOMETRICS refers to automatically recognizing an individual based on ones unique biological and behavioral traits without carrying any token and password, which significantly facilitates every aspect of our life [1][2]. As a result, in the modern society, biometric technologies have been becoming an ideal solution to the problems of a wide range of highly secure personal authentication applications [3]. So far, various biometric technologies such as face, fingerprint, iris and gait have been exhaustively investigated, and some of them have been successfully deployed [3]-[7]. As one of the most important hand-based traits, palmprint-based biometrics has also been receiving tremendous research efforts in recent

years due to its rich discriminative features such as principal lines and ridge patterns [8][9] and wide potential of real-world applications. In the past decades, a variety of palmprint recognition technologies have been investigated in the literature, such as low-resolution palmprint, high-resolution palmprint, multispectral palmprint and 3-D palmprint recognition [10]-[14]. In general, high-resolution palmprint images share highly similar ridge-based features as well as feature extraction methods such as fingerprint. Multispectral palmprint recognition refers to use and fusion of multiple models of low-resolution palmprint images for recognition [15][16]. In addition, most 3-D palmprint recognition methods converted 3-D surface information of palmprint into 2-D low-resolution palmprint images for feature extraction and recognition [13][17]. To this end, in recent years, most efforts on palmprint recognition mainly focus on low-resolution palmprint recognition [18]-[22].

In general, palmprint recognition consists of two steps of palmprint feature representation and matching [23]. The palmprint feature representation aims to exploit the discriminative features to make palmprint more separable, and the second step is to design effective classifiers to differentiate the extracted features. There is no doubt that palmprint feature representation significantly affects the performance of palmprint recognition. How to extract the discriminative features remains the crucial and challenging problem in palmprint recognition. Existing palmprint feature representation methods can be roughly grouped into categories of holistic feature and local feature representations [24]. Representative holistic feature representation methods include principal component analysis (PCA) [25], linear discriminant analysis (LDA), sparse representation (SR) [26] and deep-learning [27], which have been widely used for palmprint recognition. For example, Maadeed et al. [26] proposed a hybrid palmprint representation method by representing a query palmprint image with a sparse combination of a class-specific dictionary and a dense combination of a common intra-class variation dictionary. However, these conventional methods do not consider much and utilize the characteristics of palmprint, and their performance is still far from satisfactory. In addition, some of them are computation and memory expensive. By contrast, the typical local feature based methods generally extracted the intrinsic features of palmprint such as the principal lines and wrinkles [28]-[30]. However, the limited principal lines and messy wrinkles cannot offer acceptable performance.

It is well recognized that plenty of lines in a palmprint carry rich direction features, which are insensitive to illumination

This paper was supported in part by the National Natural Science Foundation of China under Grant 61702110, Grant 61602540, Grant 61772296 and Grant 61673175, the Shenzhen Fundamental Research fund of J-CYJ20170811155725434 and JCYJ20170412170438636, and the University of Macau MYRG2018-00053-FST.

L. Fei and B. Zhang are with the Department of Computer and Information Science, University of Macau, Taipa, Macau 999078, China (e-mail: flksxm@126.com; bobzhang@umac.mo)

Y. Xu and J. Wen are with the Bio-Computing Research Center, Harbin Institute of Technology (Shenzhen), Shenzhen 518055, China (e-mail: yongxu@yemail.com; wenjie@hrbeu.edu.cn)

Z. Guo is with the Graduate School at Shenzhen, Tsinghua University, Shenzhen 518055, China (e-mail: zhenhua.guo@sz.tsinghua.edu.cn)

W. Jia is with the School of Computer and Information, Hefei University of Technology, Hefei 230009, China (e-mail: china.jiawei@139.com)

changes. Due to this finding, most methods propose to extract and encode the direction-based features of palmprint. The most typical direction-based method was the palmcode proposed by Zhang et al. [8], which encoded the palmprint by using Gabor phase encoding scheme on a fixed direction. To better reflect the line features of palmprint, Wong et al. [31] used a bank of Gabor filters with different directions to extract the dominant direction feature of palmprint achieving promising accuracy. After that, various extended versions of the dominant direction based method were proposed, and the representative methods include fusion code [32], robust line orientation code method (RLOC) [33] and discriminative robust competitive code (DRCC) [34] methods, and so on. To completely fit the direction features of palmprint, many multiple-directions based methods were proposed. For example, Sun et al. [35] used three grouped Gaussian filters to extract direction features on three orthogonal directions. Guo et al. [36] proposed a binary orientation co-occurrence vector (BOCV) method by encoding palmprint on six directions. Fei et al. [23] proposed a double orientation code method by extracting and encoding two dominant directions. Luo et al. [37] designed a local line direction pattern representation by jointly encoding two optional directions. Zheng et al. [38] proposed a novel palmprint direction feature descriptor by computing the Difference of Vertex Normal Vectors (DoN) of a palmprint image. Moreover, more direction-based methods were comparatively studied in [22][39].

The direction-based palmprint recognition methods with promising accuracies have proved the success of the direction features for palmprint recognition [18]. However, most existing palmprint direction representations are hand-crafted and heuristics, which usually require strong prior knowledge to engineer them. Moreover, hand-crafted direction features do not represent the most discriminative direction features of palmprint. In this paper, we propose a learning-based method for discriminant palmprint direction feature extraction and recognition. We first calculate the convolution difference vector (CDV) for palmprint images as the feature container, which contain informative direction information. Then, we learn a feature mapping to project the CDV into discriminant direction binary codes (DDBC), making them have maximized variances and also maximized inter-class distance and minimized intra-class distance. Lastly, we cluster the block-wise statistics of DDBC maps forming the discriminant direction binary palmprint descriptor for palmprint recognition. Fig. 1 illustrates the basic idea of the proposed method.

The main contributions of this paper can be summarized in three fold:

- We propose a novel and informative convolution difference vector for discriminant direction feature learning. CDV can better describe the multiple dominant direction features as well as the significance of the directions. In addition, a CDV has a zero mean value and is suitable for feature learning without performing additional zero normalization.
- We propose a feature learning-based method to jointly learn and encode the discriminant and data-adaptive direction features of palmprint images. To our knowledge,

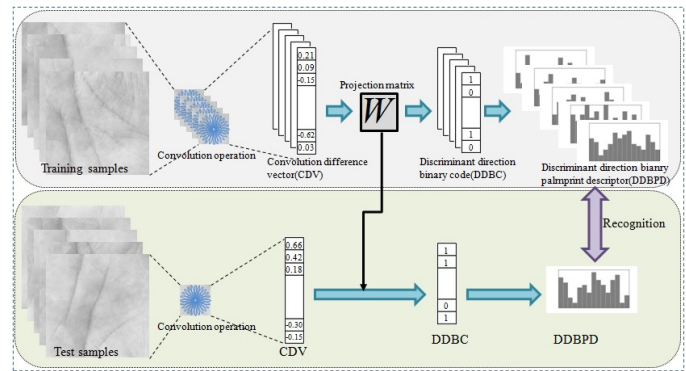


Fig. 1. The flow-chart of the proposed method. We first compute the convolution difference vector for each palmprint image. Then, we learn mapping functions, which project CDV into discriminant direction binary codes. Finally, we concatenate the block-wise histograms of DDBC into discriminant direction binary palmprint descriptor for palmprint recognition.

this is the first work with an attempt to use hash learning-based method for palmprint feature extraction and recognition.

- We conduct extensive experiments on four challenging contactless palmprint databases. Experimental results demonstrate that the proposed method is superior to state-of-the-art palmprint descriptors. The promising performance of the proposed method also validates the effectiveness of the hash learning-based method for palmprint recognition.

The rest of this paper is organized as follows. Section II introduces the related work for the preparation of the proposed method. Section III proposes a discriminant direction feature learning method for palmprint representation and recognition. Section IV presents the experimental results. Section V offers the conclusion.

II. RELATED WORK

This section briefly reviews three related topics of this paper, including the direction features of palmprint, binary coding of direction features and discriminant feature learning.

A. Direction features of palmprint

In general, since palmprint images are captured from the hands, it is inevitable that the captured images contain both the palm images and the finger parts. Therefore, the original captured palmprint images need to be preprocessed to extract the region of interest (ROI) for palmprint feature extraction and recognition. Fig. 2 shows the basic procedure of the ROI extraction.

Palmprint contains rich principal lines, wrinkles and ridge patterns, and thereby carry informative direction features. There have been extensive methods that exploited the direction features for palmprint recognition [31]-[39]. The common way of extracting palmprint direction is to define a bank of line-like templates with predesigned directions, such as Gabor filters and MFRAT, which can be used to detect the direction features of palmprint. Representative direction based methods include the competitive code method and RLOC, which extract the

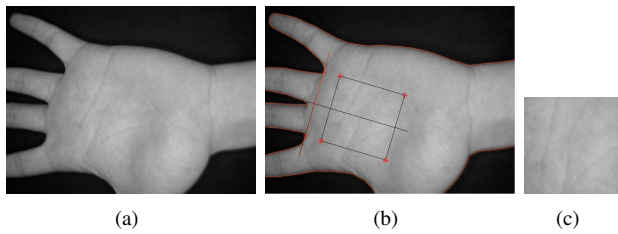


Fig. 2. The basic procedure of the ROI extraction of a palmprint image. (a) An input palmprint image; (b) The original palmprint image is first convolved with the low-pass Gaussian filter to smooth the palmprint image and then converted into a binary image by thresholding, so as to obtain the boundary of the binary image. Finally, the valley points at the bottom of the gaps between fingers are determined as the landmarks to establish a coordinate to locate a certain area; (c) The sub-image located at a certain area of a palmprint is cropped as the ROI of the palmprint image.

most dominant direction features of palmprint. They first use a bank of direction-based templates to convolve a palmprint image, and then take the direction of the template that produces the maximum direction response as the dominant direction of the palmprint. In other words, it assumes that any pixel in a palmprint image belongs to a line. The template that carries the consistent direction of the palmprint line can produce the maximum filtering response. The dominant direction of a palmprint can be extracted as follows:

$$\theta_d(I) = \arg \max_{\theta_j} \text{Resp}(T(\theta_j), I), j = 1, 2, \dots, N_\theta, \quad (1)$$

where $T(\theta_j)$ represents the templates with the directions of $\theta_j (j = 1, 2, \dots, N_\theta)$, and N_θ is the direction number of the templates. I represents a palmprint image. “*Resp*” is the line response of the templates and the palmprint image, and it usually denotes the convolution operation. θ_d represents the dominant direction feature map of the palmprint.

It is recognized that a palmprint usually contains various lines, such as cross lines and bend lines, carrying multiple direction features [36]. To this end, there have also been a number of works that proposed to exploit different kinds of direction features from palmprint. Generally, they employ a series of direction-based templates to convolve the palmprint and encode the line responses on multiple directions, but not on a single direction. A common representation of multiple direction feature extraction is as follows:

$$\theta_f(I) = f(\text{Resp}(T(\theta_j), I)), j = 1, 2, \dots, N_\theta, \quad (2)$$

where f represents a encoding function than encode the palmprint line response into direction feature codes. θ_f represents the special-designed direction feature map of the palmprint. In general, most existing palmprint direction representations are hand-crafted and thus need strong prior knowledge to engineer them.

B. Binary direction code

The binary code based feature representation has been widely used in pattern recognition work due to its high robustness and low computational complexity. There have also been extensive works that encode the direction features of palmprint into binary codes. For example, the original

competitive code method used the direction index as the feature code. To improve the computational efficiency, the competitive code method further converted the direction index code into three binary codes [31], which can be efficiently matched and thus applicable in real applications. Moreover, the binary based direction code representation shows good robustness to illumination changes [18] and image rotation of palmprint [36], which frequently affect the performance of palmprint recognition. For these reasons, the binary encoding is an effective scheme for palmprint feature representation. The widely used binary encoding schemes include thresholding operation [36] and sign function [7]. In this work, we propose a feature learning-based method to learn binary direction code for palmprint recognition.

C. Discriminant feature learning

Discriminant feature learning is to learn some mapping functions that can convert raw data into discriminative feature subspace. In recent years, a variety of discriminant feature learning methods were developed, such as the subspace-learning [40], dictionary-learning [41], transfer-learning [42], metric-learning [43] and deep-learning [27][44]. Of them, principal component analysis (PCA) and linear discriminant analysis (LDA) are ones of the most representative discriminant feature learning methods. Specifically, PCA is to learn projection functions than make the data have the maximum variances in the projected subspace. LDA is to learn a new subspace where the samples have the maximized inter-variance and meanwhile minimized intra-variances. To date, both PCA and LDA criteria have been successfully used for palmprint feature learning and recognition. For example, Ribaric et al. [45] extracted the eigenpalm features of palmprint by using the PCA principle. Wu et al. [46] proposed a fisherpalm method based on the LDA scheme for palmprint recognition. Rida et al. [47][48] proposed a hybrid palmprint recognition method by first building incoherent sample dictionary based on 2DPCA and then extracting discriminative features using 2DLDA. Most existing learning-based methods learn palmprint features from raw-pixels of palmprint images. In this work, we learn novel and discriminative direction binary features from direction-based convolution difference for palmprint recognition.

III. DISCRIMINANT DIRECTION BINARY PALMPRINT DESCRIPTOR

In this section, we first introduce the convolution difference vector of palmprint images. Then, we propose a discriminant direction binary code learning method for palmprint feature extraction and recognition.

A. Convolution difference vector

The conventional methods usually extract hand-crafted direction features of palmprint image, which require strong prior knowledge. In addition, the hand-crafted direction features may not be the optimal discriminant features of palmprint images. Based on these observations, in this paper, we propose

to learn discriminant direction features for palmprint recognition. Unlike the conventional direction-based methods that directly encode the line responses of palmprint images, we form a novel convolution difference vector for discriminant direction feature learning. We first employ a bank of direction-based templates to obtain the original convolution responses of a palmprint and then generate the CDV for discriminant direction learning. The following describes the details of the CDV.

The Gabor filter is used as the direction-based templates to extract the direction features of palmprint due to its good 2-D spectral specificity property as well as the impressive performance in palmprint recognition [31]. Specifically, we define twelve Gabor templates as [23][31] with evenly distributed directions, i.e., $\theta_j = (j - 1)\pi/12 (j = 1, 2, \dots, 12)$. For these Gabor templates, the radial frequency in radians per unit length and the standard deviation of the elliptical Gaussian are empirically set to 0.0916 and 5.6179, respectively [23][31]. Then, the convolution response between the templates and palmprint can be represented as:

$$c_j(x, y) = G(\theta_j) * I(x, y), \quad (3)$$

where $G(\theta_j)$ is the real part of the Gabor template with the direction of θ_j . “*” is the convolution operation, c represents the convolution response result and (x, y) denotes a pixel of the palmprint I . We obtain the CDV of a pixel by calculating the convolution difference between a direction and the front neighboring direction as follows:

$$CDV = [(c_1 - c_{12}), (c_2 - c_1), \dots, (c_k - c_{k-1}), \dots, (c_{12} - c_{11})]. \quad (4)$$

The size of the CDV is the direction number of the used Gabor templates. Fig. 3 shows an example of generating the CDV.

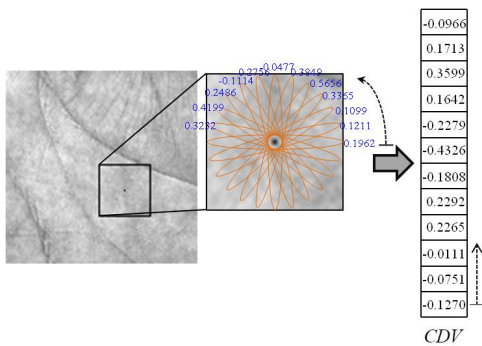


Fig. 3. An example of how to form a convolution difference vector. For any pixel of the palmprint, we convolve twelve Gabor templates with the palmprint image to obtain a bank of convolution values. Then, the convolution difference between the current direction and the front neighboring direction is computed to form the CDV.

CDV measures the convolution differences between neighboring directions so that it can better describe how direction-based convolution response changes. It can be seen that the CDV can implicitly denote the dominant direction features of palmprint. Specifically, a positive CDV data means that the convolution response on the current direction is stronger than that on the “front” neighboring direction, and a negative one denotes that its response is weaker than the “front” direction.

Hence, a positive CDV value following a negative one essentially indicates a dominant direction feature. Therefore, the multiple dominant directions of palmprint can also be precisely depicted by the CDV. Moreover, the magnitude of the CDV can represent the significance of the direction. In addition, the mean of the values within a CDV is zero, which is suitable for feature learning without extra zero normalization. Therefore, the CDV contains rich and informative direction information of a palmprint image. In this paper, we use the informative CDV to learn discriminant direction descriptor for palmprint feature representation and recognition.

B. Discriminant direction binary code learning

Due to the fact that binary features are effective and robust to local changes such as illumination and the promising effectiveness of feature extraction of hash learning [49][50][51], we aim to design a learning method to learn a bank of hash functions that can convert the CDV into discriminant direction binary codes. Specifically, given a set of training palmprint images, we first calculate the CDVs of all pixels for each palmprint image, and integrate them into a CDV matrix for the image. Then, we concatenate the CDVs of all the training palmprint images into a global training CDV matrix. Let $X = [x_1, x_2, \dots, x_N] \in R^{d \times N}$ be the global CDV matrix and x_i represents a CDV of a pixel, we aim to learn K hash functions that can convert the CDV into binary codes as follows:

$$b_i = 0.5 \times (\text{sgn}(W^T x_i) + \mathbf{1}^{K \times 1}), \quad (5)$$

where $W = [w_1, w_2, \dots, w_K] \in R^{d \times K}$ is the projection matrix, and $b_i \in \{0, 1\}^{K \times 1}$ is the binary direction code vector of a CDV. $\mathbf{1}^{K \times 1}$ is a column vector that contains K elements with the values of 1. $\text{sgn}(u)$ represents a sign function, which converts $u = [u_1, u_2, \dots, u_K]^T$ into the $\{0, 1\}^{K \times 1}$ based on the sign of each $u_i (i = 1, \dots, K)$. Specifically, for each element of u , $\text{sgn}(u_i)$ equals to 1 when $u_i > 0$, and -1 otherwise.

Inspired by the PCA and LDA criteria, in the feature space, we require that the variance of the learned binary codes is maximized. Furthermore, the learned binary codes have the maximized inter-class distance and meanwhile minimized inter-class distance. To achieve these objectives, we formulate the following objective function to learn the projection functions:

$$w_k = \arg \max_{w_k} J(w_k) = \sum_{i=1}^N \|b_{i,k} - \bar{b}_k\|^2 + 2\lambda \sum_{i=1}^N \left(\sum_{x_j \in \Omega(x_i)} \|b_{i,k} - b_{j,k}\|^2 - \sum_{x_{j'} \in \Upsilon(x_i)} \|b_{i,k} - b_{j',k}\|^2 \right), \quad (6)$$

where \bar{b}_k is the mean of the k -th binary codes of all the CDVs. Both the $\Upsilon(x_i)$ and $\Omega(x_i)$ represent the CDV sets, which have the same index as the x_i in palmprint images. In addition, the samples in $\Upsilon(x_i)$ are from the same palm as the x_i , and the samples in $\Omega(x_i)$ are from different palms. The objective function has two terms with a trade-off parameter λ . The objective of the first term is to maximize the variance of

the learned binary codes making samples more separable in an unsupervised manner. The second term is to maximize the intra-class distance and minimize the inter-class distance of the learned binary codes. The combination of these two terms aims to learn the optimal discriminant direction features of palmprint images. Fig. 4 depicts the basic procedure of the direction binary code learning of the proposed method.

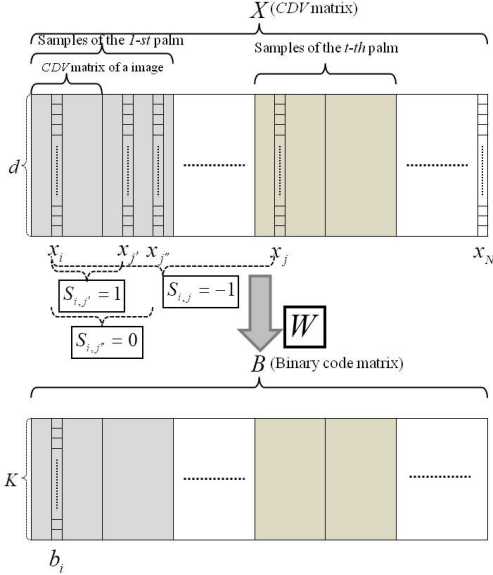


Fig. 4. An illustration of the proposed direction binary code learning model.

To optimize the objective function, we replace the l_2 -norm distance metric in the second term with the sign function multiplication, and reformulate the objective function of Eq. (6) as:

$$J(w_k) = J_1(w_k) + 2\lambda J_2(w_k) = \sum_{i=1}^N \|b_{i,k} - \bar{b}_k\|^2 + 2\lambda \sum_{i=1}^N \left(\sum_{x_{j'} \in \Upsilon(x_i)} \tilde{b}_{i,k} \times \tilde{b}_{j',k} + \sum_{x_j \in \Omega(x_i)} -(\tilde{b}_{i,k} \times \tilde{b}_{j,k}) \right), \quad (7)$$

where $\tilde{b}_{i,k} = 2b_{i,k} - 1 = \text{sgn}(w_k^T x_i)$. To our knowledge, Eq. (7) is an NP-hard problem duo to the non-linear $\text{sgn}(\cdot)$ function. According to [43][52], we can relax the $\text{sgn}(\cdot)$ function to its signed magnitude. Thus, the first term of Eq. (7) can be written in matrix form as follows:

$$J_1(W) = \|W^T X - W^T M\|^2 = \text{tr}((W^T X - W^T M)(W^T X - W^T M)^T) = \text{tr}(W^T X X^T W - 2W^T X M^T W + W^T M M^T W), \quad (8)$$

where $M = [m, m, \dots, m] \in R^{d \times N}$ be the CDV mean matrix, and $m \in R^{d \times 1}$ is the column mean vector of X . The second term can be written in a compact matrix form as:

$$J_2(W) = \frac{1}{2} \text{tr}(W^T X S X^T W), \quad (9)$$

where $S \in R^{N \times N}$ is a matrix indicating the correspondence of

X :

$$S_{p,q} = \begin{cases} 1, & \text{if } x_q \in \Upsilon(x_p), \\ -1, & \text{if } x_q \in \Omega(x_p), \\ 0, & \text{else.} \end{cases} \quad (10)$$

For example, in Fig. 4, $S_{i,j'} = 1$, $S_{i,j} = -1$ and $S_{i,j''} = 1$. As a result, the two criterions in the objective function can be combined as:

$$J(W) = J_1(W) + 2\lambda J_2(W) = \text{tr}(W^T X X^T W - 2W^T X M^T W + W^T M M^T W) + \lambda \text{tr}(W^T X S X^T W) = \text{tr}(W^T (X X^T - 2X M^T + M M^T + \lambda X S X^T) W) = \text{tr}(W^T Q W), \quad (11)$$

where $Q = X X^T - 2X M^T + M M^T + \lambda X S X^T$. Therefore, the objective function can be rewritten as:

$$W = \arg \max_W J(W) = \arg \max_W \text{tr}(W^T Q W), \quad \text{subject to: } W^T W = I. \quad (12)$$

Mathematically, Eq. (12) can be solved by finding the maximum variance directions of Q , which is a typical eigenvalue problem. $W = [w_1, w_2, \dots, w_K]$ is the matrix that comprises of the eigen-vectors corresponding to the top K eigen-values of Q .

After the projection matrix W is obtained, a bank of discriminant direction binary codes can be obtained for each pixel of a palmprint. In other word, the proposed method can extract at most K binary feature code maps for a palmprint image. Fig. 5 shows some examples of the learned direction binary feature code maps of the first to six levels. It can be seen that the different levels of DDBC can extract different kinds of binary features



Fig. 5. The learned discriminant direction feature maps. The first image is a palmprint image. The second to seven ones are the learned DDBC maps of the first to six levels, respectively.

C. DDBC-based palmprint descriptor

Palmprint images have obviously position-specific direction features. For example, the principal lines and wrinkles of palmprint have obvious direction features and comparatively some flat region has superficial direction features. To address this, we propose to use the block-wise statistics of DDBC as palmprint representation. Specifically, we first learn the DDBC features from a palmprint image. Previous studies [31][36] have shown that six binary codes can achieve encouraging performance. Inspired by this finding, in this paper, we extract six DDBCs for each pixel of palmprint images, unless otherwise stated. Then, we encode the binary feature DDBC codes of each CDV into a real value. Third, we divide the DDBC feature map into non-overlapping blocks, and compute the DDBC histograms for these blocks. Finally, all the DDBC block-wise

features within the same palmprint are concatenated as the global feature vector, named as discriminant direction binary palmprint descriptor (DDBPD). Algorithm 1 summarizes the procedure of the proposed method.

Algorithm 1 DDBPD

Input: Training sample set $X = [x_1, x_2 \dots x_n]$, parameter λ , binary code length K , a new palmprint image y .

Output: Feature mapping matrix W , the feature descriptor of y

- 1: Forming the CDVs of X and y
- 2: Calculating the mapping matrix W based on the CDVs of X using Eq. (12)
- 3: Computing binary feature codes of y based on W using Eq. (5)
- 4: Forming the block-wise histogram-based feature descriptor of y
- 5: **return** W and feature descriptor of the palmprint image y .

In palmprint recognition, the similarity of two DDBPDs can be measured by using the chi-square distance metric. Fig. 6 illustrates the pipeline of the DDBPD-based representation and matching. In this paper, the local block size is empirically set to 16×16 pixels.

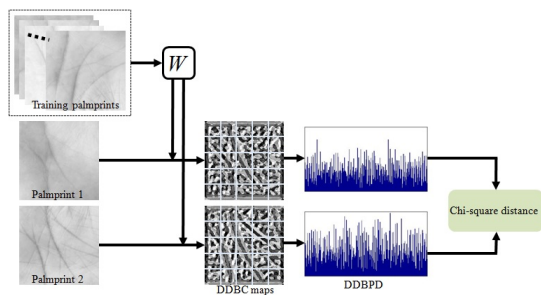


Fig. 6. The pipeline of DDBPD-based palmprint representation and matching.

IV. EXPERIMENTAL RESULTS

In this section, we evaluate the proposed DDBPD method via extensive experiments on the four challenging contactless palmprint image databases, including the CASIA, IITD, TJU and HFUT databases. The CASIA and IITD databases are employed to show the effectiveness of the proposed method on palmprint identification, and the large-scale TJU and HFUT databases are used to test the proposed method for palmprint verification. All experiments were conducted on a PC with double-core Intel(R) i7-7700 (3.60GHz), RAM 16.00 GB and MATLAB 8.3.0 in Windows 10.0 operating system. In the following, we show the detailed experiments and the results on each database.

A. Databases

The CASIA palmprint database [53] contains 5,502 palmprint images captured from 312 subjects, who provided 8 to 17 palmprint images for each palm. All of the palmprint

images were captured by using a normal CMOS camera fixed on a specific-developed device without restricting the posture and position of palms. Note that two individuals provided no palmprint images in the CASIA database. In addition, a palmprint image was wrongly labeled. As a result, we reformed the CASIA database with 5501 palmprint samples collected from 310 subjects of 620 different palms to conduct the experiments.

The IITD palmprint database [55] consists of 2,601 palmprint images collected from 230 subjects of 460 different palms. Each palm provided 5 to 6 palmprint images. Exceptionally, one palm contained 7 palmprint images. All the samples from the database were captured by a normal camera in an indoor environment with circular fluorescent illumination around the camera lens.

The TJU palmprint database [26] consist of 12,000 palmprint images collected from 300 volunteers of 600 different palms, including 192 males and 108 females. The samples of each individual were collected in two sessions with an average interval of about 61 days. 10 palmprint images were captured from a palm in each session, and thus 20 palmprint images were contributed for a palm in two sessions. All samples were captured in a specific-devised device with free variations in pose, rotation, scale and palm opening-degree.

The HFUT palmprint image database [18] contains 16,000 palmprint images collected from 400 individuals with 800 different palms. All samples were captured in two sessions with an interval of around 10 days. Each palm of an individual provided 10 palmprint images in one session, and thus an individual provided totally 40 samples for both the left and right palms in two sessions. Therefore, the HFUT databases consist of 800 different palms of palmprint images and each palm contains 20 samples. To the best of our knowledge, the HFUT is the largest contactless palmprint image database.

Table I tabulates the basic information of the four palmprint databases. In the following experiments, we use the ROI segmentation method [8] to extract the ROIs of all palmprint images and resize them into 64×64 pixels. Fig. 7 shows some typical palmprint images selected from the four different databases as well as the corresponding ROIs. It can be seen that all samples captured under relatively free environments have large intra-class variations in pose, rotation and translation.

TABLE I
DESCRIPTIONS OF THE CASIA, IITD, TJU AND HFUT PALMPRINT DATABASES.

Database	Total image number	Individual number	Palm number	Image per palm
CASIA	5,501	310	620	8~17
IITD	2,601	230	460	5~7
TJU	12,000	300	600	20
HFUT	16,000	400	800	20

B. Experiments on the CASIA database

In this experiment, we first form a training sample set by evenly selecting different samples per each palm and use the

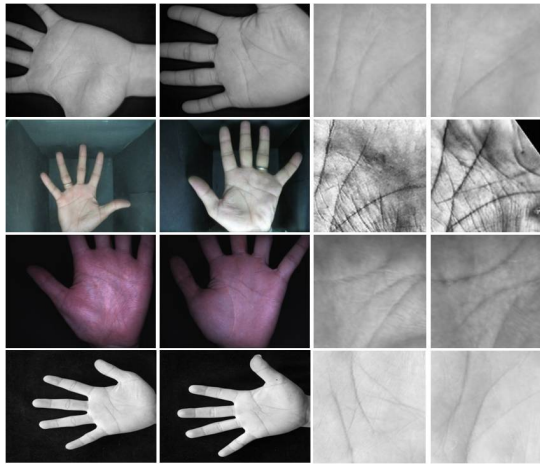


Fig. 7. Some typical palmprint images selected from four different palmprint databases. The first to fourth rows show the samples selected from the CASIA, IITD, TJU and HFUT databases, respectively. For each row, the first two images are the original captured palmprint samples and the last two images are the corresponding ROIs.

rest as probe samples. Then, we perform projection functions learning on the training sample set and apply the learned projections on both the training set and probe set for feature extraction. Lastly, we perform feature identification based on nearest neighbor classifier. In this study, we form four training sample sets by selecting k palmprint images from each palm as the training samples and the rest as the test samples. Specifically, we select the first k images from each palm, that are the $\{1, 2, \dots, k\}$ -th samples of the palm, to form the first training sample set. We select the last k palmprint images, that are the $\{n-k+1, n-k+2, \dots, n\}$ -th samples, from each palm forming the second training set. In addition, the third training set selects the $\{1 \times \text{step}, 2 \times \text{step}, \dots, k \times \text{step}\}$ -th palmprint images from each palm, where “ n ” is the total sample number of a palm and “ $\text{step} = \text{floor}(n/k)$ ”. The fourth training set consists of the $\{n - k \times \text{step} + 1, n - (k - 1) \times \text{step} + 1, \dots, n - \text{step} + 1\}$ -th palmprint images of each palm. k is respectively set as 3 and 4. For each training set, we calculate the average identification accuracies for the corresponding probe set. We empirically set λ in DDBC learning model as 0.1, and the DDBC number as 6.

To better evaluate the proposed method, the popular feature descriptor such as LBP and state-of-the-art direction-based palmprint descriptors, including the competitive code [31], ordinal code [35], E-BOCV [39], fast competitive code (Fast-Comp) [20], LLDP [37], HOL [22], DoN [38] and DRCC [34], were implemented. In addition, the recently published holistic feature-based methods including the CR_Compcode [26] and E-SRC [48] were also executed. It is noted that both HOL and LLDP have different implementations. Since different versions of them achieve comparable performance, in this study, we implemented the HOL algorithm based on Gabor filter and implemented the LLDP algorithm based on the MFRAT template with the LDN encoding scheme, respectively.

The proposed DDBPD method learns the discriminant features from the CDV container. To show the distance between the DDBPD and the CDV, we directly encode each CDV of

a palmprint image into binary code features by using sign function for palmprint recognition. Specifically, each CDV is encoded into twelve binary codes so that a palmprint image can be converted into twelve binary code maps. Then, the NN classifier with hamming distance is used for feature identification.

Table II summarizes the rank-one identification accuracies and the standard errors of different palmprint descriptors based on different number of training samples (#Tr). It can be seen from the table that the proposed method can achieve higher identification accuracies than the state-of-the-art direction-based palmprint descriptors. This is because our DDBPD learns and encodes the data-adaptive discriminative directions of palmprint as features when compared with the existing hand-crafted descriptors. Compared with the LBP representation, the DDBPD is elaborately designed for discriminative palmprint feature extraction, so that better recognition performance is obtained. In addition, the CDV-based palmprint descriptor cannot achieve comparable accuracies as the conventional direction-based methods such as the competitive code and ordinal code. The possible reason is that the CDV-based descriptor simply encodes the CDV values without any feature learning and selection. Any code map of the CDV-based descriptor with low discriminability possibly reduces the performance of the CDV-based descriptor. However, the promising performance of the DDBPD method demonstrates that the CDV can provide informative data for discriminant feature learning for palmprint recognition.

TABLE II
THE RANK-ONE IDENTIFICATION ACCURACIES AND STANDARD ERRORS (%) OF DIFFERENT METHODS ON THE CASIA DATABASE.

#Tr	k=3	k=4
CDV	78.7147±10.1303	82.8958±9.3751
LBP	73.2079±8.6587	76.6220±8.7438
Competitive code	82.2370±8.9281	85.9235±7.8811
Ordinal code	80.5822±9.2164	84.5747±8.4951
E-BOCV	82.1890±9.1595	85.6670±8.2822
FastComp	82.1065±8.6790	85.5511±1.8606
CR_CompCode	85.6015±6.6451	87.2973±6.6287
E-SRC	82.0022±3.2431	84.9851±3.2685
LLDP	94.0632±2.9975	95.1437±2.6391
HOL	89.3677±5.7950	91.6414±4.8414
DoN	82.5935±7.5359	86.6396±8.8935
DRCC	84.9973±7.5017	88.2241±6.5620
DDBPD	95.4958±2.8050	96.4085±2.6860

The DDBC learning model contains one balancing parameter, i.e., λ . To evaluate the affects of the parameter on discriminative feature learning, we test the performance of the model with different values of λ . Specifically, we set λ as 0.001, 0.01, 0.1, 1, 10, 100 and 1000, respectively, based on which we learn the projection matrix on the aforementioned training sets. Then, we perform palmprint identification on the corresponding probe sets and calculate the average recognition rates, as shown in Fig. 8. It can be seen that the proposed method achieves the optimal recognition performance when λ is set to 0.1 and 1. In addition, the proposed method can achieve comparable performance for different λ , showing good robustness to the parameter.

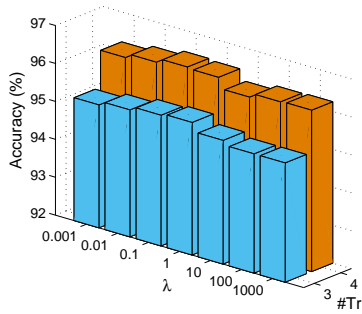


Fig. 8. The average rank-one identification accuracies of the proposed method based on different values of λ on the CASIA database.

For the proposed method, the CDV is calculated on twelve directions and thus the CDV size is 12. Thus, at most twelve DDBC's can be learned for a point on a palmprint. In this section, we test the performance of the DDBPD with different DDBC numbers from 1 to 12, respectively. Fig. 9 depicts the average identification accuracies of the proposed DDBPD method on the aforementioned probe sample sets. It can be seen that the recognition rate of the proposed method is rapidly increased when the DDBC number increases from 1 to 6. After that, the recognition rate is slowly improves. It is noted that using more DDBC's will increase the size of the DDBPD as well as the computational time. It is observed that the DDBPD with DDBC numbers of 6 and 7 can achieve close to the optimal recognition rate. Thus, we can set DDBC number as 6 to balance the recognition performance and the size of the DDBPD.

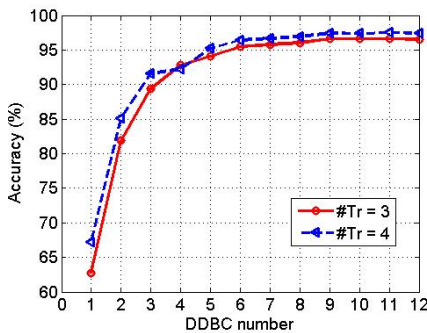


Fig. 9. The average rank-one identification accuracies of the proposed method using different number of DDBC on the CASIA database.

C. Experiments on the IITD database

In this experiment, we form two training sample set groups by evenly selecting k samples per each palm as the training sample sets, where $k = 2$ and $k = 3$, respectively. For $k = 3$, the training sample set group contains four training sets which are formed as the same scheme as subsection IV.B. For the training sample set group with $k = 2$, we form four training sets by selecting the $\{1, 1 + step\} - th$, $\{2, 2 + step\} - th$, $\{n - step - 1, n - 1\} - th$ and $\{n - step, n\} - th$ samples from each palm, respectively, where “ n ” is the total sample

number of the palm and “ $step = floor(n/k)$ ”. Similar to the comparison on CASIA, we also compared the proposed method with LBP and state-of-the-are palmprint descriptors. Table III lists the average rank-one identification accuracies of different methods based on these training sample sets. It is clearly seen that the proposed method outperforms the LBP descriptor and the representative direction-based palmprint recognition methods. This is possibly because our proposed DDBPD is a data-adaptive feature representation of palmprint images.

TABLE III
THE RANK-ONE IDENTIFICATION ACCURACIES AND STANDARD ERRORS (%) OF DIFFERENT METHODS ON THE IITD DATABASE.

#Tr	k=2	k=3
LBP	60.8268±1.8719	62.4898±4.3353
Competitive code	81.3801±0.2524	84.7257±2.7770
Ordinal code	79.2981±0.3699	82.8624±2.9090
E-BOCV	86.0351±0.4355	88.5340±2.3222
FastComp	82.3171±0.3308	85.8518±2.8928
CR_CompCode	86.8828±0.8545	87.7969±2.5146
E-SRC	79.6508±4.2402	85.5872±3.1437
LLDP	93.7646±0.8193	94.8231±1.2276
HOL	91.7609±1.0536	92.6290±1.9416
DoN	81.7458±4.1719	84.8764±3.3412
DRCC	85.9176±7.4503	88.7797±2.7677
DDBPD	95.3599±0.3699	96.4373±1.1079

To evaluate the affects of the tradeoff parameter λ , we set it with different values as 0.001, 0.01, 0.1, 1, 10, 100 and 1000, respectively, and conduct palmprint identification. The average rank-one identification accuracies on the aforementioned sample sets are shown in Fig. 10. It is seen that the proposed method with $\lambda = 0.1$ and $\lambda = 0.01$ achieves the best accuracy. Based on the experimental results and previous comparisons in subsection IV.B, we empirically set $\lambda = 0.1$ in this paper.

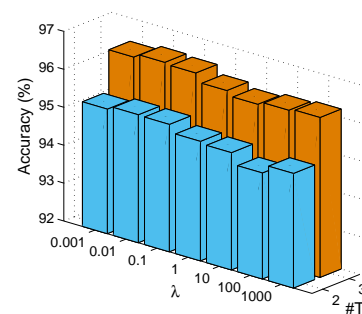


Fig. 10. The average rank-one identification accuracies of the proposed method based on different values of λ on the IITD database.

Moreover, to find the optimal number of DDBC, we conduct palmprint identification by using the proposed method with different number of DDBC. Fig. 11 depicts the identification result, which shows that the accuracy of the proposed method is rapidly increasing at the beginning and slowly later. The accuracies of the proposed method are very close to the best when DDBC number is larger than 6, which is consistent to the previous findings in subsection IV.B. In general, the DDBC number exactly determines the size of the DDBPD, and thus

heavily affects to the computational time cost. To balance the accuracy and calculation burden, it is optimal to set the DDBC number as 6 or 7 for the proposed method.

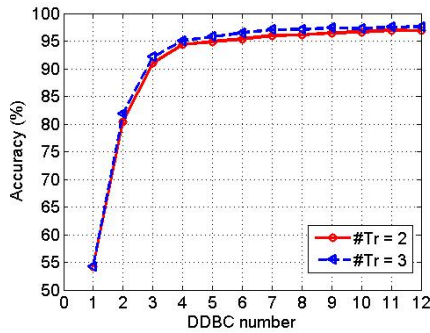


Fig. 11. The average rank-one identification accuracies of the proposed method using different number of DDBC on the IITD database.

D. Experiments on the TJU database

In this section, we use the TJU database to evaluate the performance of the proposed method on palmprint verification. We follow the evaluation protocol in [26], which used the samples captured in the first session forming the gallery sample set and the samples of the second session forming the probe sample set. Thus, both the gallery and probe sample sets contain 6,000 palmprint images. We first learn the projection functions on the gallery set. Then, we apply these functions on both gallery and probe samples for feature extraction. In the matching stage, we use the Chi-square distance to compute the similarity of two descriptors.

In our verification experiments, each palmprint image in the probe set is to match against all the samples from the gallery set. If two matched palmprint images are from the same palm, the matching of the two samples is named as a genuine match; otherwise, defined as an impostor match. Then, we calculate the false acceptance rate (FAR) and genuine acceptance rate (GAR) to evaluate the proposed method. Fig. 12 shows the ROC curves of FAR versus GAR obtained by the proposed DDBPD method and the representative direction-based palmprint recognition methods. For our DDBPD, we respectively use 6 (dotted red line) and 7 (solid red line) DDBCs to form the palmprint descriptors. Table IV lists the GARs of these methods under the same settings of FAR=0.001 and FAR=0.1. It is clearly seen that the proposed method can achieve better performance than the compared methods, demonstrating the effectiveness of the proposed DDBPD method on palmprint verification.

In addition, Table V tabulates the identification accuracies of these methods on the TJU database. It shows that the proposed method with seven DDBCs can achieve the best accuracy on the TJU database.

E. Experiments on the HFUT database

In the experiment, the palmprint images captured in the first session, which are the first 10 images of a palm, are used to form the gallery set. Correspondingly, the rest palmprint

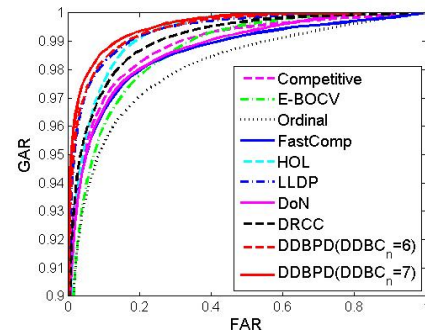


Fig. 12. ROC curves of different methods on TJU database.

TABLE IV
THE GAR(%) WITH FAR=0.001 AND FAR=0.1 OF DIFFERENT METHODS ON THE TJU DATABASE.

	GAR (FAR=0.001)	GAR (FAR=0.1)
Competitive code	85.1633	97.1150
Ordinal code	82.8283	95.3750
E-BOCV	77.9633	96.2586
FastComp	85.3350	96.6100
LLDP	86.3650	98.2550
HOL	82.0633	97.8717
DoN	84.9673	96.6836
DRCC	85.7150	97.2817
DDBPD(DDBC _n =6)	88.2900	98.4800
DDBPD(DDBC _n =7)	90.0517	98.6583

images collected in the second session are used as the probe samples. Each probe sample is matched with all the samples in the gallery set, and the GAR and FAR are computed. The ROC of the proposed method and the representative direction-based methods are shown as in Fig. 13. The corresponding GAR on FAR=0.001 and FAR=0.1 are listed in Table VI. It is seen that the proposed method with DDBC=6 (dotted red line) and DDBC=7 (solid red line) outperforms most of the existing methods. In particular, the proposed DDBPD with DDBC=7 can achieve the best GAR among the six compared methods under the same FAR settings.

Moreover, Table VII tabulates the identification results of the above compared methods on the HUFT methods. It shows that the proposed method with DDBC=7 can achieve the best identification performance than the other compared methods.

TABLE V
THE RANK-ONE IDENTIFICATION ACCURACIES (%) OF DIFFERENT METHODS ON THE TJU DATABASE.

Methods	Identification rate
Competitive code	96.2333
Ordinal code	96.2000
E-BOCV	96.8333
FastComp	97.1500
CR_CompCode	98.4833
E-SRC	96.4500
LLDP	98.5000
HOL	95.2833
DoN	95.8333
DRCC	97.2500
DDBPD(DDBC _n =6)	97.8333
DDBPD(DDBC _n =7)	98.7333

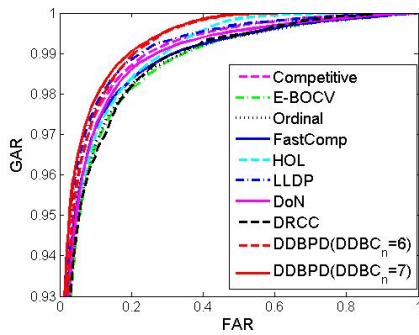


Fig. 13. ROC curves of different methods on the HUFT database.

TABLE VI
THE GAR(%) WITH FAR=0.001 AND FAR=0.1 OF DIFFERENT METHODS ON THE HFUT DATABASE.

	GAR (FAR=0.001)	GAR (FAR=0.1)
Competitive code	83.1738	97.4963
Ordinal code	82.2825	96.8138
E-BOCV	77.3800	87.9900
FastComp	83.2825	97.3550
LLDP	83.1850	97.8375
HOL	82.8525	97.0300
DoN	80.4075	97.3125
DRCC	75.9000	95.9125
DDBPD(DDBC _n =6)	80.9675	97.5450
DDBPD(DDBC _n =7)	83.3450	98.0238

F. Noisy palmprint recognition

In practical applications, contactless palmprint images are usually captured under open and free environments. This means there is an inevitability that the captured palmprint images suffer from some noise due to the influences of external environment, image capture device and image processing. In this subsection, we simulate the noisy palmprint images by adding noise on the existing palmprint images to test the performance of the proposed method. Specifically, we add the Gaussian noise with the mean of 0 and the variance of 5 on the images of the CASIA and TJU palmprint database, to form two synthetic noisy palmprint image datasets. Fig. 14 shows some typical samples of the synthetic noisy palmprint images.

TABLE VII
THE RANK-ONE IDENTIFICATION ACCURACY (%) OF DIFFERENT METHODS ON THE HFUT DATABASE.

Methods	Identification rate
Competitive code	96.9750
Ordinal code	97.0625
E-BOCV	93.1250
FastComp	96.9125
CR_CompCode	96.7675
E-SRC	96.2750
LLDP	97.2500
HOL	95.9000
DoN	96.5125
DRCC	97.5750
DDBPD(DDBC _n =6)	97.4875
DDBPD(DDBC _n =7)	97.8625

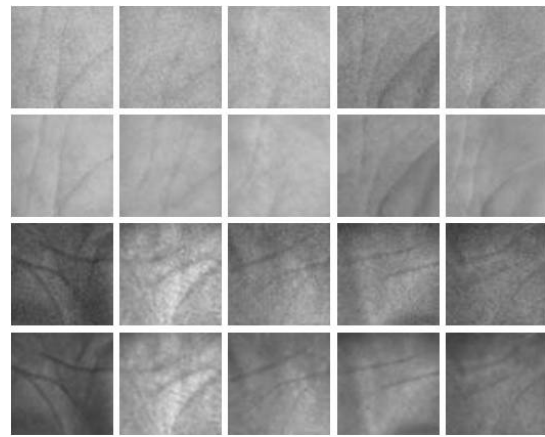


Fig. 14. The examples of the noisy palmprint images. The images of the first row are the noisy palmprint images corresponding to the samples of the second row selected from the CASIA database. The images of the third row are the noisy palmprint images corresponding to the samples of the fourth row selected from the of the TJU database.

Then, we follow the protocols of subsections IV.B and IV.D to conduct palmprint identification experiments on the noisy CASIA and noisy TJU datasets, respectively. Table VIII tabulates the identification results of different methods on these two noisy palmprint image datasets. It can be seen that for each dataset the accuracy of each method is lower than that on the original palmprint database. In addition, the proposed method always achieves a higher accuracy than the ten compared method on each dataset. This demonstrates the effectiveness of the proposed method for feature learning of noisy palmprint images.

TABLE VIII
THE EXPERIMENTAL RESULTS OF DIFFERENT METHODS ON THE NOISY CASIA AND TJU PALMPRINT DATASETS.

Methods	Noisy CASIA	Noisy TJU
Competitive code	79.7515±9.6379	95.7167
Ordinal code	76.7715±10.4422	95.4833
E-BOCV	79.3464±10.2956	96.2000
FastComp	80.0948±9.3644	96.5833
CR_CompCode	82.8108±7.1210	95.9667
E-SRC	80.9852±6.6868	95.7000
LLDP	89.4809±5.7044	97.0167
HOL	74.2928±8.4390	92.0167
DoN	80.2359±10.1584	95.4000
DRCC	83.4523±8.2040	96.8000
DDBPD(DDBC _n =6)	89.7281±5.6344	96.4333
DDBPD(DDBC _n =7)	90.1813±5.4713	97.3167

G. Discussion and computational complexity

The above comparative experimental results demonstrate the proposed method achieves the best performance than state-of-the-art palmprint descriptors on both palmprint identification and verification. This is because the proposed method automatically learns the discriminative features from informative direction container, namely convolution difference vectors of palmprint images. By contrast, the conventional palmprint descriptors extract hand-craft direction features from the raw-data of palmprint images. Moreover, the promising recognition

accuracy achieved by the proposed method demonstrates the feasibility of the hash learning-based methods on palmprint recognition.

Compared with the existing hand-craft based methods, the proposed method needs to learn a bank of projection functions for discriminative direction feature extraction. To solve the DDBC learning model, a relation matrix S needs to be constructed. The size of S is proportional to the size of palmprint images and the training sample number. Suppose there are n images in the training set and each palmprint has p pixels, the size of S is $(p \times n)^2$, and thus S is possible to be a very large matrix. Note that S is a sparse matrix containing a large number of zeros, and the positions of both 1 and -1 can be easily indicated. Therefore, we do not need to construct the matrix in real calculation. Instead, we directly sum up the values of these positions indicated by 1 and -1 in the matrix, which could significantly reduce the memory storage and computational time.

To test the computational cost of the proposed method, we form a training sample set containing 100 samples and computed the computation time of the feature extraction and identification. Table IX shows the average feature extraction and identification time of 100 query samples based on different methods. The projection functions learning time of the proposed method is about 52 s. It is seen that the proposed method takes a little more feature extraction time than other methods. This is because the proposed method uses more direction-based templates than the conventional methods. In addition, the proposed method constructs CDV for feature extraction and the conventional methods extract features from raw-data. Note that the projection function learning of the proposed method and the feature extraction of the training samples can be performed offline in real applications. Therefore, the efficiency of palmprint recognition heavily depends on the feature matching time. It can be seen that DDBPD has a fast matching speed and a complete identification time of a query sample is less than 0.03 s, which is acceptable for real-world applications.

TABLE IX
THE AVERAGE FEATURE EXTRACTION AND IDENTIFICATION TIME (S) OF DIFFERENT METHODS.

Methods	Feature extraction	Identification
Competitive code	0.0126	0.0040
Ordinal code	0.0068	0.0204
E-BOCV	0.0134	0.0346
LLDP	0.0206	0.0034
DDBPD	0.0265	0.0020

V. CONCLUSION

In this paper, we propose a new direction binary code learning method for palmprint representation and recognition. We first form informative convolution difference vectors from palmprint images, and then learn discriminant direction binary codes from CDV. Finally, we pool the global block-wise DDBC histograms as feature representation, namely discriminant direction binary palmprint descriptor, for palmprint recognition. Experimental results on four benchmark contactless

palmprint databases demonstrate that the proposed method achieves better recognition performance than state-of-the-art palmprint descriptors. The reasonable good performance of the proposed method also validates the effectiveness and feasibility of the hash learning-based methods for palmprint recognition. As the proposed method is a general feature learning method, it is reasonable and interesting to apply the DDBPD to other hand-based biometrics tasks such as dorsal-hand-vein and finger-knuckle-print recognition to further demonstrate its effectiveness. In addition, how to apply the DDBPD model to further learn the discriminant features from the existing hand-crafted palmprint descriptors such as the competitive code seems to be another interesting direction.

REFERENCES

- [1] Q. Tao, R. Veldhuis, "Biometric Authentication System on Mobile Personal Devices," IEEE Transaction on Instrumentation and Measurement, vol. 59, no. 4, pp. 763–773, 2010.
- [2] A. K. Jain, A. Ross, S. Prabhakar, "An introduction to biometric recognition," IEEE Transactions on Circuits and Systems for Video Technology, vol. 14, no. 1, pp. 4–20, 2004.
- [3] D. Zhang, "Advanced pattern recognition technologies with applications to biometrics," Medical Information Science Reference, 2009.
- [4] A. K. Jain, "K. Nandakumar, A. Ross, 50 years of biometric research: Accomplishments, challenges, and opportunities," Pattern Recognition Letters, vol. 79, no. 1, pp. 80–105, 2016.
- [5] G. Jaswal, A. Kaul, R. Nath, "Knuckle Print Biometrics and Fusion Schemes-Overview, Challenges, and Solutions," ACM Computer Survey, vol. 49, no. 2, pp. 34–79, 2016.
- [6] D. Huang, C. Shan, M. Ardabilian, "Local Binary Patterns and Its Applications to Facial Image Analysis: A Survey," IEEE Transactions on Systems, Man, and Cybernetics - Part C: Applications and Reviews, vol. 41, no. 6, pp. 765–781, 2011.
- [7] A. Kong, D. Zhang, M. Kamel, "A survey of palmprint recognition," Pattern Recognition, vol. 42, no. 7, pp. 1408–1418, 2009.
- [8] D. Zhang, W-K. Kong, J. You, M. Wong, "Online Palmprint Identification," IEEE Transactions on Pattern Analysis and Machine Intelligence, vol. 25, no. 9, pp. 1041–1050, 2003.
- [9] A. K. Jain, J. Feng, "Latent Palmprint Matching," IEEE Transactions on Pattern Analysis and Machine Intelligence, vol. 30, no. 6, pp. 1032–1047, 2009.
- [10] L. Fei, G. Lu, W. Jia, S. Teng, D. Zhang, "Feature Extraction Methods for Palmprint Recognition: A Survey and Evaluation," IEEE Transactions on Systems, Man, and Cybernetics: Systems, vol. 49, no. 2, pp. 346–363, 2019.
- [11] D. Zhang, Z. Guo, G. Lu, L. Zhang, W. Zuo, "An Online System of Multi-spectral Palmprint Verification," IEEE Transactions on instrumentation and measurement, vol. 59, no.2, pp. 480–490, 2010.
- [12] M. D. Bounneche, L. Boubchir, A. Bouridane, B. Nekhou, A. A. Cherif, "Multi-spectral palmprint recognition based on oriented multiscale log-Gabor filters," Neurocomputing, vol. 205, pp. 274–286, 2016.
- [13] L. Fei, G. Lu, W. Jia, J. Wen, D. Zhang, "Complete Binary Representation for 3D Palmprint Recognition," IEEE Transactions on Instrumentation and Measurement, vol. 67, no. 12, pp. 2761–2771, 2018.
- [14] G. Li, J. Kim, "Palmprint recognition with Local Micro-structure Tetra Pattern," Pattern Recognition, vol. 61, pp. 29–46, 2017.
- [15] J. Dai, J. Feng, J. Zhou, "Robust and Efficient Ridge-Based Palmprint Matching," IEEE Transactions on Pattern Analysis and Machine Intelligence, vol. 34, no. 8, pp. 1618–1632, 2012.
- [16] J. Dai, J. Zhou, "Multifeature-Based High-Resolution Palmprint Recognition," IEEE Transactions on Pattern Analysis and Machine Intelligence, vol. 33, no. 5, pp. 945–957, 2011.
- [17] W. Li, D. Zhang, L. Zhang, G. Lu, J. Yan, "3-D Palmprint Recognition With Joint Line and Orientation Features," IEEE Transactions on System, Man, and Cybernetics, Part C: Applications and Reviews, vol. 41, no. 2, pp. 274–279, 2011.
- [18] W. Jia, B. Zhang, J. Lu, Y. Zhu, Y. Zhao, W. Zuo, H. Ling, "Palmprint Recognition Based on Complete Direction Representation," IEEE Transaction on Image Processing, vol. 26, no. 9, pp. 4483–4498, 2017.

- [19] A. Kumar, "Towards More Accurate Matching of Contactless Palmprint Images under Less Constrained Environments," *IEEE Transactions on Information Forensics and Security*, DOI 10.1109/TIFS.2018.2837669, pp. 1–13, 2018.
- [20] Q. Zheng, A. Kumar, G. Pan, "Suspecting Less and Doing Better: New Insights on Palmprint Identification for Faster and More Accurate Matching," *IEEE Transactions on Information Forensics and Security*, vol. 11, no. 3, pp. 633–641, 2016.
- [21] D. Zhong, X. Du, K. Zhong, "Decade progress of palmprint recognition: a brief survey," DOI: 10.1016/j.neucom.2018.03.081, *Neurocomputing*, 2018.
- [22] W. Jia, R. X. Hu, Y. K. Lei, "Histogram of Oriented Lines for Palmprint Recognition," *IEEE Transactions on Systems, Man, and Cybernetics: Systems*, vol. 44, no. 3, pp. 385–395, 2014.
- [23] L. Fei, Y. Xu, W. Tang, D. Zhang, "Double-orientation code and non-linear matching scheme for palmprint recognition," *Pattern Recognition*, vol. 49, no. 1, pp. 89–101, 2016.
- [24] D. Zhang, W. Zuo, F. Yue, "A Comparative Study of Palmprint Recognition Algorithms," *ACM Computing Survey*, vol. 44, no. 1, pp. 1–37, 2012.
- [25] S. A. Maadeed, X. Jiang, I. Rida, A. Bouridane, "Palmprint identification using sparse and dense hybrid representation," *Multimedia Tools and Applications*, DOI: 10.1007/s11042-018-5655-8, pp. 1–15, 2018.
- [26] L. Zhang, L. Li, A. Yang, Y. Shen, M. Yang, "Towards contactless palmprint recognition: A novel device, a new benchmark, and a collaborative representation based identification approach," *Pattern Recognition*, vol. 69, no. 1, pp. 199–212, 2017.
- [27] S. Minaee, Y. Wang, "Palmprint Recognition Using Deep Scattering Convolutional Network," *arXiv preprint arXiv:1603.09027*, pp. 1–13, 2016.
- [28] D. S. Huang, W. Jia, D. Zhang, "Palmprint verification based on principal lines," *Pattern Recognition*, vol. 41, no. 4, pp. 1316–1328, 2008.
- [29] X. Wu, D. Zhang, K. Wang, "Palm Line Extraction and Matching for Personal Authentication," *IEEE Transactions on Systems, Man, and Cybernetics, Part A: Systems and Humans*, vol. 36, no. 5, pp. 978–987, 2006.
- [30] D. Palma, P. L. Montessoro, G. Giordano, F. Blanchini, "Biometric Palmprint Verification: A Dynamical System Approach," *IEEE Transactions on Systems, Man, and Cybernetics: Systems*, DOI: 10.1109/TSM-C.2017.2771232, pp. 1–12, 2018.
- [31] A. Kong, D. Zhang, "Competitive Coding Scheme for Palmprint Verification," in: *Proceeding of International Conference on Pattern Recognition*, 2004, pp. 520–523.
- [32] A. Kong, D. Zhang, M. Kamal, "Palmprint identification using feature-level fusion," *Pattern Recognition*, vol. 39, no. 3, pp. 478–487, 2006.
- [33] W. Jia, D. Huang, D. Zhang, "Palmprint verification based on robust line orientation code," *Pattern Recognition*, vol. 41, no. 1, pp. 1504–1513, 2008.
- [34] Y. Xu, L. Fei, J. Wen, D. Zhang, "Discriminative and Robust Competitive Code for Palmprint Recognition," *IEEE Transactions on Systems, Man and Cybernetics: Systems*, vol. 48, no. 2, pp. 232–241, 2018.
- [35] Z. Sun, T. Tan, Y. Wang, S. Li, "Ordinal Palmprint Representation for Personal Identification," in: *Proceeding of International Conference on Computer Vision and Pattern Recognition*, 2005, pp. 279–284.
- [36] Z. Guo, D. Zhang, L. Zhang, W. Zuo, "Palmprint verification using binary orientation co-occurrence vector," *Pattern Recognition Letters*, vol. 30, no. 1, pp. 1219–1227, 2009.
- [37] Y. Luo, L. Zhao, B. Zhang, W. Jia, F. Xue, J. Lu, Y. Zhu, B. Xu, "Local line directional pattern for palmprint recognition," *Pattern Recognition*, vol. 50, pp. 26–44, 2016.
- [38] Q. Zheng, A. Kumar, G. Pan, "A 3d feature descriptor recovered from a single 2d palmprint image," *IEEE Transactions on Pattern Analysis and Machine Intelligence*, vol. 38, no. 6, pp. 1272–1279, 2016.
- [39] L. Zhang, H. Li, J. Niu, "Fragile Bits in Palmprint Recognition," *IEEE Signal processing letters*, vol. 19, no. 10, pp. 663–666, 2012.
- [40] J. Wen, X. Fang, J. Cui, L. Fei, K. Yan, Y. Chen, Y. Xu, "Robust Sparse Linear Discriminant Analysis," *IEEE Transactions on Circuits and Systems for Video Technology*, DOI: 10.1109/TCSVT.2018.2799214, pp. 1–13, 2018.
- [41] T. Ivana, P. Frossard, "Dictionary learning," *IEEE Signal Processing Magazine*, vol. 28, no. 2, pp. 27–38, 2011.
- [42] L. Zhang, D. Zhang, "Robust Visual Knowledge Transfer via Extreme Learning Machine-Based Domain Adaptation," *IEEE Transactions on Image Processing*, vol. 25, no. 10, pp. 4959–4973, 2016.
- [43] J. Lu, V. E. Liong, X. Zhou, J. Zhou, "Learning Compact Binary Face Descriptor for Face Recognition," *IEEE Transactions on Pattern Analysis and Machine Intelligence*, vol. 37, no. 10, pp. 2041–2056, 2015.
- [44] J. Svoboda, J. Masci, M. M. Bronstein, "Palmprint recognition via discriminative index learning," in: *Proceeding of International Conference on Pattern Recognition*, 2016, pp. 4232–4237.
- [45] S. Ribaric, I. Fratric, "A Biometric Identification System Based on Eigenpalm and Eigenfinger Features," *IEEE Transactions on Pattern Analysis and Machine Intelligence*, vol. 27, no. 11, pp. 1698–1709, 2005.
- [46] X. Wu, D. Zhang, K. Wang, "Fisherpalms based palmprint recognition," *Pattern Recognition Letter*, vol. 24, pp. 2829–2838, 2003.
- [47] I. Rida, R. Herault, G. Marcialis, G. Gasso, "Palmprint recognition with an efficient data driven ensemble classifier," *Pattern Recognition Letters*, DOI: 10.1016/j.patrec.2018.04.033, pp. 1–7, 2018.
- [48] I. Rida, S. A. Maadeed, A. Mahmood, A. Bouridane, S. Bakshi, "Palmprint identification using an ensemble of sparse representations," *IEEE ACCESS*, vol. 6, no. 1, pp. 3241–3248, 2018.
- [49] J. Wang, T. Zhang, J. Song, N. Sebe, H. Shen, "A Survey on Learning to Hash," *IEEE Transactions on Pattern Analysis and Machine Intelligence*, vol. 40, no. 4, pp. 769–790, 2018.
- [50] J. Lu, V. Liong, J. Zhou, "Simultaneous Local Binary Feature Learning and Encoding for Homogeneous and Heterogeneous Face Recognition," *IEEE Transactions on Pattern Analysis and Machine Intelligence*, vol. 40, no. 8, pp. 1979–1993, 2018.
- [51] Z. Lai, J. Wu, W. K. Wong, F. Shen, "Jointly Sparse Hashing for Image Retrieval," *IEEE Transactions on Image Processing*, vol. 27, no. 12, pp. 6147–6158, 2018.
- [52] J. Wang, S. Kumar, S. F. Chang, "Semi-Supervised Hashing for Scalable Image Retrieval," in: *Proceeding of International Conference on Computer Vision and Pattern Recognition*, 2010, pp. 3424–3431.
- [53] CASIA palmprint image database, <http://biometrics.idealtest.org/>.
- [54] T. Ojala, M. Pietikainen, T. Maenpaa, "Multiresolution Gray-Scale and Rotation Invariant Texture Classification with Local Binary Patterns," *IEEE Transactions on Pattern Analysis and Machine Intelligence*, vol. 24, no. 7, pp. 971–987, 2002.
- [55] A. Kumar, S. Shekhar, "Personal Identification Using Multibiometrics Rank-Level Fusion," *IEEE Transactions on Systems, Man, and Cybernetics-Part C: Applications and Reviews*, vol. 41, no. 5, pp. 743–752, 2011.